

# Coating Thickness Effect on the Cyclic Performance of Aluminum and Zirconium Metal-Organic Frameworks for Heat Pump Application

Ibrahim Albaik<sup>1\*+</sup>, Kamal Diab<sup>1,2+</sup>, Raya Al-Dadah<sup>1</sup>, Saad Mahmoud<sup>1</sup>, Mohamed A. Ismail<sup>3,4</sup>

<sup>1</sup> Department of Mechanical Engineering, University of Birmingham, Edgbaston, Birmingham B15 2TT, UK

<sup>2</sup> Nanoscience Department, Institute of Basic and Applied Sciences, Egypt-Japan University of Science and Technology, New Borg El-Arab City, Alexandria 21934, Egypt

<sup>3</sup>Department of Chemical Engineering, College of Engineering, King Khalid University, Abha 61411 Kingdom of Saudi Arabia

<sup>4</sup>Institute of Engineering Research and Materials Technology, National Center for Research, Khartoum 2424, Sudan

\*Corresponding Author

+Authors contributed equally to this work

## ABSTRACT

Metal-organic framework (MOF) is a promising adsorbent material to replace the conventional ones for many applications such as cooling and desalination. In this study, we report the effect of coating thicknesses using binder-agent aqueous solution-based synthesis strategy on the cyclic performance of aluminum and zirconium MOFs. The results showed that the coated MOFs enhances the cyclic performance over the neat granular and powdered forms. Moreover, the maximum effective coating thickness that provides faster cycle time compared to the neat adsorbent material is 0.85mm in aluminum MOF (aluminum fumarate), while it is 1.1mm in zirconium MOF (MOF-801). The enhancement of the coating thickness on the heat pump application is also studied.

**Keywords:** Metal organic framework, aluminum fumarate, MOF-801 and water uptake.

## NONMENCLATURE

### Abbreviations

MOF	Metal-Organic Framework
COP	Coefficient of Performance
DVS	Dynamic vapor sorption
BET	Brunauer–Emmett–Teller

## 1. INTRODUCTION

The adsorption systems provide an alternative solution toward an efficient and environmental friendly heat-driven cooling and desalination system over the conventional systems such as; the compression refrigeration cycle as a cooling system [1] and the Reverse Osmosis technology as a desalination system [2]. These systems consumes a relatively high electrical power and produce high CO<sub>2</sub> emissions [2], while the adsorption system can be operated using waste heat energy from the industry or solar energy [3–5]. However, the adsorption systems are still under development in order to deliver a higher coefficient of performance (COP) compared to the conventional systems, which will gain more investors' attention if this goal is achieved.

Many studies have enhanced the system performance through improving the adsorber bed design to increase the heat and mass transfer to/from the adsorbent material [6–8], while other researches focused to improve the adsorbent material properties such as decrease the heat of adsorption, increase the water uptake (the water capacity of the adsorbent material at different relative pressure in equilibrium condition), enhance the effective thermal conductivity and deliver a fast water kinetics [9,10]. Additionally, the method of applying the adsorbent material inside the adsorber bed by packing it between the tube fins of the

heat exchanger [11] or coating it on the heat exchanger surfaces also plays a significant role in improving the heat and mass transfer, which ultimately improve the performance of the adsorption system [12]. Packing the adsorbent material has a major drawback in the thermal conductivity and thermal contact resistance between the material and the heat exchanger surfaces, which increase the heat transfer resistance through the adsorbent material.

Recently, a huge effort have been dedicated to minimize the thermal contact resistance with lower reduction in internal and external mass transfer of the vapour through the adsorbent material, since reducing the heat transfer resistance is directly linked to an increase in the mass transfer resistance. Coating the adsorbent material is a promising candidate to eliminate the contact resistance and speed up the water kinetics in the adsorbent material. Several techniques are considered in coating, which can be summarized through *situ* direct synthesis or binder agents [13]. In *situ* direct synthesis, the adsorbent material is directly crystallized onto the heat exchanger surfaces, which can reduce the heat and mass transfer resistances and cycle time (adsorption and desorption). The mass transfer resistance is very limited since the coating thickness is very thin (less than 0.1mm), which makes the adsorption system has a very low COP due to the high metal-adsorbent mass ratio. This technique produces a coating layer with 100% of adsorbent material without adding any binder, which makes it uniform and compact [13]. Scaling up this technique is facing technical manufacturing limitations, which is difficult to be applied in widespread applications [14]. On the other hand, binder-based coating produces a reproducible thicknesses by forming an adherent films which considered simple method compared to direct synthesis [15,16]. Moreover, this method eliminates the thermal contact resistance with the heat exchanger surfaces and enhance the effective thermal conductivity while it causes a reduction in porosity of the composite structure. Several studies were carried out to identify the coating thickness and the binder agent percentage, especially with organic framework materials (MOF), since these materials have higher surface area compared to the conventional adsorbent material [17](silica gel and zeolite) which can overcome the reduction in porosity after adding the binder agent. Therefore, more studies need to be investigated to maximize the coating thickness to reduce the metal-adsorbent mass ratio in order to be applied in different applications such as

water desalination and cooling. In this study, a detailed investigation of the coating thickness effect on the cyclic performance were carried out to obtain the effective coating thickness using different MOF materials (Alumnum Fumarate (AlFum) and MOF-801), which represents a strong tool that can be applied in the adsorption system to achieve higher COP.

## 2. MATERIAL AND METHODS

Zirconium oxychloride octahydrate ( $ZrOCl_2 \cdot 8H_2O$ , purity  $\geq 99.8\%$ ), N,N-dimethylformamide (DMF) (HPLC grade), fumaric acid (purity  $\geq 99\%$ ), Al-fum was purchased from MOF-Technology Co. Anhydrous DMF and formic acid (purity  $\geq 99.8\%$ ) were obtained from sigma Aldrich. Ethanol (HPLC grade) and hydroxyethyl cellulose were purchased from Fisher Scientific. All chemicals obtained were used without further purification. Pyrex screw-capped bottles were used for synthesis, solvent exchange and storage.

Nitrogen ( $N_2$ ) adsorption isotherms were recorded on  $N_2$  adsorption and desorption isotherms were measured on a Micromeritics Tristar II at 77 K. A liquid  $N_2$  bath was used for the measurements at 77 K. Before each run, samples were activated at 120 °C for 18 h under high vacuum. Water isotherms and cyclic performance tests were measured using dynamic vapour sorption apparatus (DVS).

**Synthesis of MOF-801,  $Zr_6O_4(OH)_4(\text{fumarate})_6$ :** In a 500 mL screw- capped jar, 1.16 g (50 mmol) of fumaric acid and 3.2 g (50 mmol) of  $ZrOCl_2 \cdot 8H_2O$  were dissolved in a mixed solvent of DMF and formic acid (40 mL and 14 mL, respectively). The solvent mixture was then heated in a conventional oven at 120°C overnight to produce powder MOF-801 as a white precipitate. The precipitate was collected by centrifuge at 10,000 rpm and washed three times with 100 mL DMF, then three times with 100 mL ethanol and subsequently dried in oven at 40°C. The air-dried MOF sample was transferred to a vacuum oven at 120°C for 12 hours, yielding activated MOF-801 as a white powder (yield: 2.1 g). This batch was further used to determine the water sorption characteristic curves and Brunauer–Emmett–Teller (BET) isotherms for adsorption and desorption.

**Synthesis of coating films of MOF-801 and Al-Fum:** To prepare 10 % binder solution of MOF-801 or Al-Fum (see **Figure 1 (a-c)**), in a 500 mL beaker, 1 g of binder powder (hydroxyethyl cellulose) was fully dissolved in 50

ml water to get a viscous solution of binder using stirrer for 15 minutes at 80°C. Afterwards, 10 g of MOF powder was fully dispersed in the viscous solution of binder using sonication for 5 minutes. These procedures are presented in **Figure 1 (d-g)**. Then, the viscous solution of MOF/binder was dip-coated on slides of aluminum foil as shown in **Figure 1 (h)**. The MOF coated aluminum slides were left in the oven at 120°C to form a homogenous layer of MOF for 30 minutes, then another layer of MOF/binder solution could be dip-coated on the dried layer to tune the thickness of MOF coated layers. **Figure 1 (i)** shows different thicknesses of MOFs that are ready for characterizations.

### 3. RESULTS AND DISCUSSIONS

In order to assess the microporosity of powder material and the different coating thicknesses of MOF-801 (0.3, 0.5 and 1.1mm) and AlFum (0.3 and 1.1mm) layers with binder, the nitrogen sorption isotherms were measured for MOF-801 powder, AlFum powder and their thicknesses. The isotherms of MOF-801 and AlFum MOF

with their different thicknesses showed type-I like isotherms as shown in **Figure 2**. This observation indicated the maintained microporosity even after adding binder to the MOF powder. AlFum powder demonstrated a BET surface area of 635 m<sup>2</sup>/g while its composite with 10 % binder was 510 and 280 m<sup>2</sup>/g for 0.3 and 1.1 mm thicknesses respectively as shown in **Figure 2 (a)**. The decrease in BET surface area could be attributed to the effect of binder in blocking the pores of AlFum powder. Moreover, a noticeable decrease of surface area in case of 1.1 mm thickness may be attributed to the difficulty of nitrogen gas to access the internal pores of this relatively high thickness. On the other hand, the surface area for MOF-801 powder, 0.3, 0.5 and 1.1 mm MOF-801 layer thicknesses demonstrated a BET surface area of 900, 870 , 850 and 720 m<sup>2</sup>/g respectively, **Figure 2 (b)** . Since the composite contained about 10 wt % of binder, the observed decreased surface area of the composite reflected the mass contribution of cellulose binder which is noticeable in composite materials. However, at 1.1 mm thickness,



Figure 1. Optical images for MOFs coating synthesis. (a) AlFum-powder, (b) binder, (c) MOF-801 – powder, (d, e) binder solution preparation, (f, g) MOF/binder solution preparation, (h) dip coating MOFs on aluminum foil with different thicknesses and (i) MOFs different thicknesses ready for characterizations after drying

MOF-801 still provides a decent surface area since the probability of blocking the pores in case of MOF-801 is lower than AlFum. This might be justified by the large pore volume in AlFum compared to MOF-801 which makes it easy to be blocked.

diameter of 0.4-0.8mm shows an adsorption and desorption times of 55 and 30 minutes (cycle time of 85 minutes). While in powder form, the cycle time is slightly decreased to 75 minutes. The powder form has better permeability compared to the granular one which eases

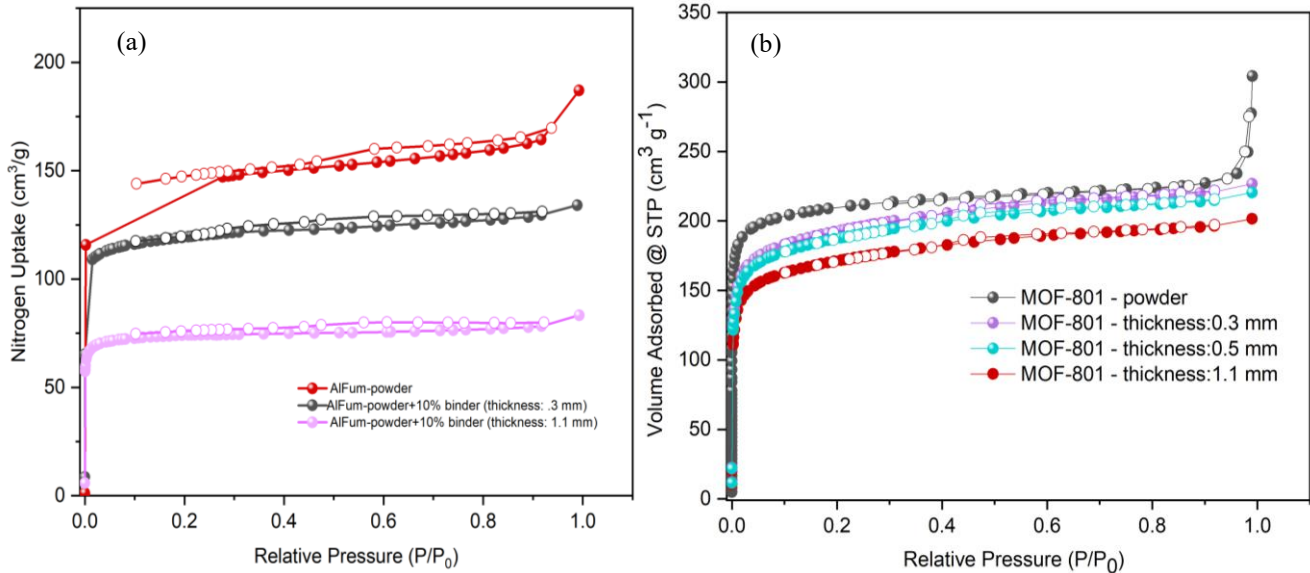


Figure 2. BET nitrogen isotherms of (a) AlFum and (b) MOF-801- (neat powder, and powder with binder at different thicknesses)

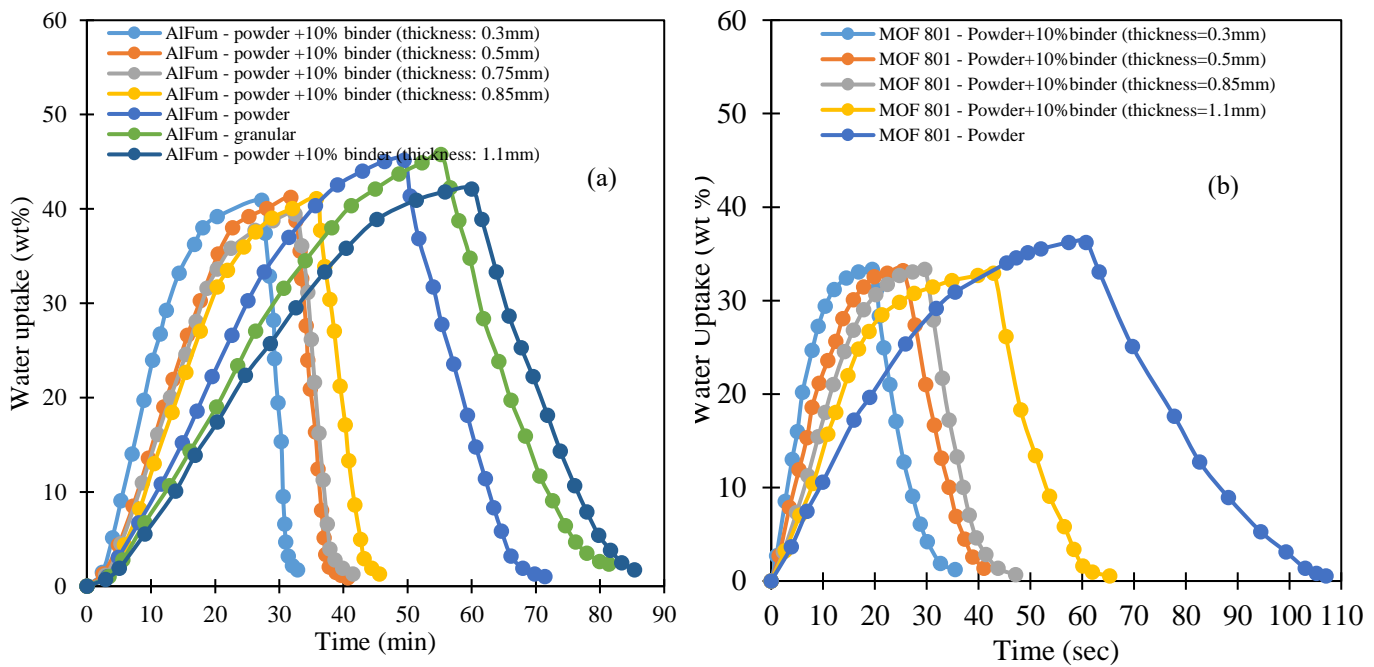


Figure 3. Water cyclic performance at relative pressure of 90% and heating temperature of 90°C using DVS (a) AlFum and (b) MOF-801- (neat powder, neat granular, and powder with binder at different thicknesses)

DVS device is used to test the cyclic performance of the neat MOFs (powder or granular) and mixed MOFs with 10% binder at different thicknesses at relative pressure of 90% and heating temperature of 90°C as shown in **Figure 3**. AlFum granular with circular particle

the mass transfer of the water vapor through the adsorbent material. However, the powder form cannot be applied in the application unless mixed with binder agent. After adding 10% of binder agent to the AlFum, the cycle time shows a dramatical reduction to 30

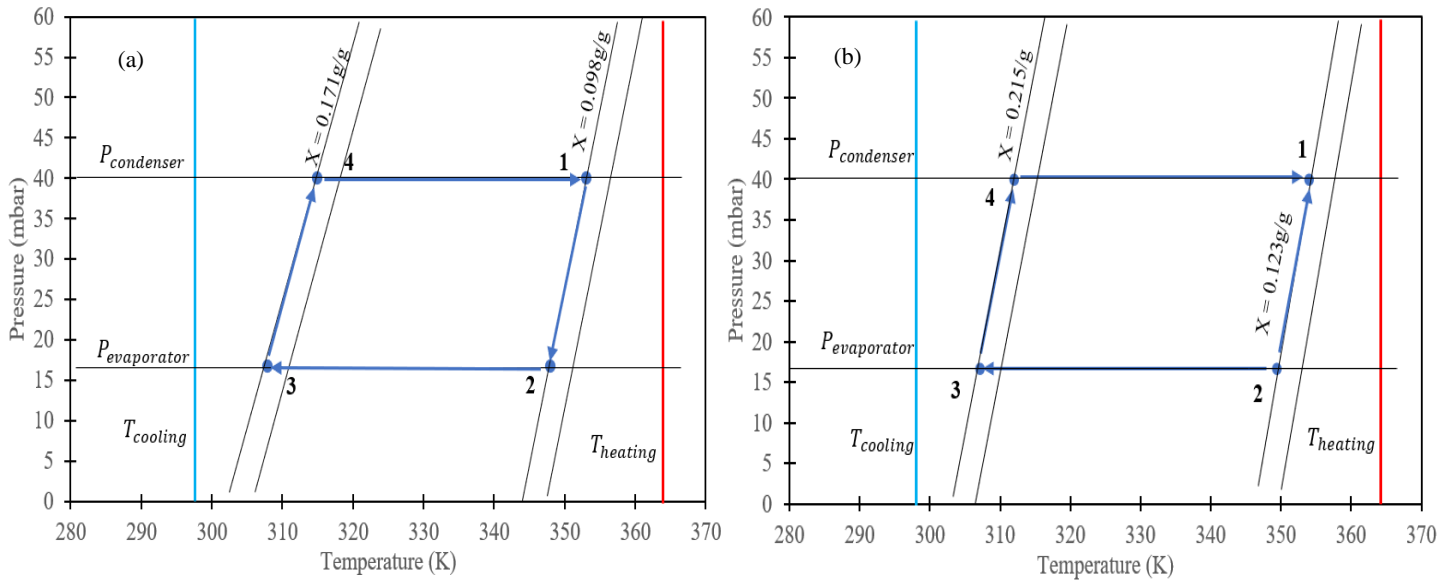


Figure 4. PTX diagram of Heat pump adsorption system using (a) MOF 801 powder and (b) MOF 801 powder with 10% binder (thickness:0.85mm) –  $T_{heating} = 90^{\circ}\text{C}$ ,  $T_{cooling} = 25^{\circ}\text{C}$ ,  $T_{chilled} = 23^{\circ}\text{C}$  and  $t_{halfcycle} = 300$  sec

minutes at coating thickness of 0.3mm followed by 35, 45 and 50 minutes at thicknesses of 0.5, 0.75 and 0.85mm respectively as shown in **Figure 3 (a)**. Any further increase in the thickness causes a very high mass transfer resistance which leads to increase the cycle time to be higher than the neat AlFum at thickness of 1.1mm. Note that mixing binder agent with AlFum causes a slight decrease in the maximum water uptake from 45 to 39 wt %. On the other hand, in neat powdered form of MOF-801, the adsorption and desorption time are 60 and 47 minutes (cycle time of 107 minutes), which are higher than the cycle time of AlFum in powder form. Different thicknesses are also applied after mixing the binder with MOF-801 (0.3, 0.5, 0.85, and 1.1mm) as shown in **Figure 3 (b)**. It is observed that the cycle time at thickness of 1.1mm is still providing a better cyclic performance compared to the neat MOF with a cycle time of 65 minutes. In contrary, AlFum with coating thickness of 1.1mm is no longer effective since the neat MOF-801 has smaller pore volume and larger surface area compared to the purchased AlFum, which makes it capable to have good cyclic performance at thicker coating thickness.

To investigate the coating thickness effect on the performance of adsorption application, heat pump adsorption system is used which consists of adsorber bed, evaporator and condenser. The pressure-temperature-water uptake (PTX) diagram of the heat pump is shown in **Figure 4**. When MOF 801 in powder form is used without binder, the water uptake is increased from 0.098 to 0.171 g/g using a half cycle time of 300 seconds, while adding binder with a coating

thickness of 0.85mm increase the water uptake between the desorption and adsorption process from 0.123 to 0.215 g/g. This indicates that the cooling effect that can be obtained from the system using this thickness is higher than the neat MOF.

#### 4. CONCLUSIONS

Toward the practical implementation of the aluminum and zirconium metal-organic framework (MOF) materials in cooling and desalination applications, a facile and effective strategy were developed for MOF coating on heat exchanger surfaces using binder agent. Different coating thicknesses were investigated using Brunauer–Emmett–Teller (BET) and dynamic vapor sorption (DVS) devices in order to be compared with the neat MOFs. Despite the slight reduction in the maximum water uptake as a result of mixing the adsorbent material with 10% of binder agent, it provides more than two cycles (adsorption and desorption) in 75 minutes using coating thicknesses of 0.3 and 0.5 mm, while only one cycle can be performed during this period when neat MOF is used. At coating thicknesses of thicker than 0.85 and 1.1mm in aluminum fumarate and MOF-801 respectively, this coating strategy is no longer effective since a significant impact on the porosity and surface area is observed. This finding will allow us to implement a thicker coating thicknesses in the adsorption systems, which will lead to increase the coefficient of performance since the metal-adsorbent mass ratio will be decreased.

## 5. REFERENCES

- [1] Almasri RA, Abu-Hamdeh NH, Esmail KK, Suyambazhahan S. Thermal solar sorption cooling systems, a review of principle, technology, and applications. *Alexandria Eng J* 2022;61:367–402. <https://doi.org/10.1016/j.aej.2021.06.005>.
- [2] Youssef PG, Al-Dadah RK, Mahmoud SM. Comparative analysis of desalination technologies. *Energy Procedia* 2014;61:2604–7. <https://doi.org/10.1016/j.egypro.2014.12.258>.
- [3] Hamdy M, Askalany AA, Harby K, Kora N. An overview on adsorption cooling systems powered by waste heat from internal combustion engine. *Renew Sustain Energy Rev* 2015;51:1223–34. <https://doi.org/10.1016/j.rser.2015.07.056>.
- [4] Wang RZ, Pan QW, Xu ZY. Solar-powered adsorption cooling systems. *Adv Sol Heat Cool* 2016:299–328. <https://doi.org/10.1016/B978-0-08-100301-5.00012-6>.
- [5] Fernandes MS, Brites GJVN, Costa JJ, Gaspar AR, Costa VAF. Review and future trends of solar adsorption refrigeration systems. *Renew Sustain Energy Rev* 2014;39:102–23. <https://doi.org/10.1016/j.rser.2014.07.081>.
- [6] Wang Y, Li M, Ji X, Yu Q, Li G, Ma X. Experimental study of the effect of enhanced mass transfer on the performance improvement of a solar-driven adsorption refrigeration system. *Appl Energy* 2018;224:417–25. <https://doi.org/10.1016/j.apenergy.2018.05.017>.
- [7] Solmuş I, Yamali C, Yildirim C, Bilen K. Transient behavior of a cylindrical adsorbent bed during the adsorption process. *Appl Energy* 2015;142:115–24. <https://doi.org/10.1016/j.apenergy.2014.12.080>.
- [8] Albaik I, Al-Dadah R, Mahmoud S, Solmaz İ. Non-equilibrium numerical modelling of finned tube heat exchanger for adsorption desalination/cooling system using segregated solution approach. *Appl Therm Eng* 2021;183. <https://doi.org/10.1016/j.applthermaleng.2020.116171>.
- [9] Elsayed E, Al-Dadah R, Mahmoud S, Anderson P, Hassan A, Youssef P. Numerical investigation of MIL-101(Cr)/GrO composite performance in adsorption cooling systems. *Energy Procedia* 2017;142:4131–7. <https://doi.org/10.1016/j.egypro.2017.12.336>.
- [10] Ming Y, Chi H, Blaser R, Xu C, Yang J, Veenstra M, et al. Anisotropic thermal transport in MOF-5 composites. *Int J Heat Mass Transf* 2015;82:250–8. <https://doi.org/10.1016/j.ijheatmasstransfer.2014.11.053>.
- [11] Zhang LZ. A three-dimensional non-equilibrium model for an intermittent adsorption cooling system. *Sol Energy* 2000;69:27–35. [https://doi.org/10.1016/S0038-092X\(00\)00010-4](https://doi.org/10.1016/S0038-092X(00)00010-4).
- [12] Elsayed E, Saleh MM, Al-Dadah R, Mahmoud S, Elsayed A. Aluminium fumarate metal-organic framework coating for adsorption cooling application: Experimental study. *Int J Refrig* 2021;130:288–304. <https://doi.org/10.1016/j.ijrefrig.2021.05.015>.
- [13] Capri A, Frazzica A, Calabrese L. Recent developments in coating technologies for adsorption heat pumps: A review. *Coatings* 2020;10:1–24. <https://doi.org/10.3390/coatings10090855>.
- [14] Calabrese L. Anticorrosion behavior of zeolite coatings obtained by in situ crystallization: A critical review. *Materials (Basel)* 2018;12. <https://doi.org/10.3390/ma12010059>.
- [15] van Heyden H, Munz G, Schnabel L, Schmidt F, Mintova S, Bein T. Kinetics of water adsorption in microporous aluminophosphate layers for regenerative heat exchangers. *Appl Therm Eng* 2009;29:1514–22. <https://doi.org/10.1016/j.applthermaleng.2008.07.001>.
- [16] Dawoud B. Water vapor adsorption kinetics on small and full scale zeolite coated adsorbents; A comparison. *Appl Therm Eng* 2013;50:1645–51. <https://doi.org/10.1016/j.applthermaleng.2011.07.013>.
- [17] Furukawa H, Cordova KE, O’Keeffe M, Yaghi OM. The chemistry and applications of metal-organic frameworks. *Science (80- )* 2013;341. <https://doi.org/10.1126/science.1230444>.

## ACKNOWLEDGEMENT

The authors extend their appreciation to the Deputyship for Research & Innovation, Ministry of Education in Saudi Arabia for funding this research work through the project number 969.